Precision Engineering 33 (2009) 408–417

Contents lists available at ScienceDirect

Precision Engineering

journal homepage: www.elsevier.com/locate/precision

On-line diagnostics in the Mobile Spatial coordinate Measuring System (MScMS)

Fiorenzo Franceschini*, Maurizio Galetto, Domenico Maisano, Luca Mastrogiacomo

Politecnico di Torino, Dipartimento di Sistemi di Produzione ed Economia dell'Azienda (DISPEA), Corso Duca degli Abruzzi 24, 10129 - Torino, Italy

ARTICLE INFO

Article history:
Received 14 January 2008
Received in revised form 8 September 2008
Accepted 8 November 2008
Available online 3 December 2008

Keywords:
Mobile measuring system
Coordinate metrology
Dimensional measurements
Large-scale metrology
Wireless-sensor-networks
Localization algorithms
On-line diagnostics

ABSTRACT

Mobile Spatial coordinate Measuring System (MScMS) is a wireless-sensor-network based system developed at the industrial metrology and quality engineering laboratory of DISPEA – Politecnico di Torino. It has been designed to perform simple and rapid indoor dimensional measurements of large-size volumes (large-scale metrology).

It is made up of three basic parts: a "constellation" of wireless devices (Crickets), a mobile probe, and a PC to store and elaborate data. Crickets and mobile probe utilize ultrasound (US) transceivers in order to evaluate mutual distances.

The system makes it possible to calculate the position – in terms of spatial coordinates – of the object points "touched" by the probe. Acquired data are then available for different types of elaboration (determination of distances, curves or surfaces of measured objects).

In order to protect the system against causes of error such as, for example, US signal diffraction and reflection, external uncontrolled US sources (key jingling, neon blinking, etc.), or software non-acceptable solutions, MScMS implements some statistical tests for on-line diagnostics. Three of them are deeply analyzed in this paper: "energy model-based diagnostics", "distance model-based diagnostics", and "sensor physical diagnostics". For each measurement, if all these tests are satisfied at once, the measured result may be considered acceptable with a specific confidence coefficient. Otherwise, the measurement is rejected.

After a general description of the MScMS, the paper focuses on the description of these three on-line diagnostic tools. Some preliminary results achieved by the system prototype are also presented and discussed.

1. Introduction

In many industrial fields (for example, automotive and aerospace) dimensional measurements of large-size objects should be easily and rapidly taken [1–5]. Nowadays, the problem can be handled using many metrological systems, based on different technologies (optical, mechanical, electromagnetic, etc.). These systems are more or less adequate, depending on measuring conditions, user's experience and skill, cost, accuracy, portability, etc. In general for measuring medium–large-size objects, portable systems can be preferred to fixed ones. Transferring the measuring system to the measured object place is often more practical than the vice-versa [1].

This paper analyzes the Mobile Spatial coordinate Measuring System (MScMS), which has been developed at the industrial metrology and quality engineering laboratory of DISPEA – Politecnico di Torino [6].

MScMS is a wireless-sensor-network based system, designed to perform dimensional measurements of medium–large-size objects (for example, longerons of railway vehicles, airplane wings, fuselages, etc.). These objects can hardly be measured by traditional coordinate measurement systems, such as, for example, Coordinate Measurement Machines (CMMs) because of their limited working volume [7,1]. MScMS working principle is very similar to that of well-known NAVSTAR GPS (NAVigation Satellite Timing And Ranging Global Positioning System) [8]. The main difference is that MScMS is based on ultrasound (US) technology to evaluate spatial distances, instead of radiofrequency (RF). MScMS is easily adaptable to different measuring environments and does not require complex procedures for installation, start-up or calibration [6].

The aim of this paper is to describe the on-line diagnostics tools implemented in the system in order to continuously monitor measurement reliability.

2. The concept of "reliability of a measurement"

If we refer to the field of CMMs, the concept of "on-line metrological performance verification" is strictly related to the notion of

* Corresponding author. Tel.: +39 011 5647224; fax: +39 011 5647299.
E-mail address: fiorenzo.franceschini@polito.it (F. Franceschini).

0141-6359/$ – see front matter © 2008 Elsevier Inc. All rights reserved.
doi:10.1016/j.precisioneng.2008.11.003

"on-line self-diagnostics" [5,9]. In a same sense, this approach is "complementary" to that of uncertainty evaluation [10–15]. In general, the on-line measurement verification is a guarantee for the preservation of a measurement system characteristics (including accuracy, repeatability, and reproducibility) [16,17]. The effect of a measuring system degradation is the production of "non-reliable measurements".

In general, we can define the concept of "reliability of a measurement" as follows.

For each measurable value *x*, we can define an acceptance interval [*LAL*, *UAL*] (where *LAL* stands for Lower Acceptance Limit, and *UAL* for Upper Acceptance Limit):

$$LAL \le x \le UAL$$

The measure *y* of the quantity *x*, produced by a given measurement system, is considered "reliable" if

$$LAL \le y \le UAL$$

From the point of view of a measurement system, the I and II type probability errors (misclassification rates) respectively correspond to

$$\alpha = Pr\{y \notin [LAL, UAL] | LAL \le x \le UAL\}$$
$$\beta = Pr\{LAL \le y \le UAL | x \notin [LAL, UAL]\}$$

Usually *LAL* and *UAL* are not a priori known.

The acceptance interval is defined considering the metrological characteristics of the measurement system (accuracy, reproducibility, repeatability, etc.), as well as the required quality level of the measurement result [16,17].

The problem of system "on-line self-diagnostics" is not a recent matter and many strategies have been proposed in various fields [18–20]. In the most critical sectors, such as the aeronautical and nuclear ones, where there is an absolute need to promptly detect every malfunctions, the typical approach is based on "physical redundancy". Principally it consists of instrumentation and system control device replication. Although being effective, this method can affect system cost and complexity [9].

An alternative and/or complementary method to physical redundancy is the "model-based redundancy" (also called "analytical redundancy"). This approach substitutes the replication of a physical instrumentation by the use of appropriate mathematical models. These latter may derive from physical laws applied to experimental data or from self-learning method (for example, neural networks). This kind of diagnostics allows the detection of system failures by means of the comparison between measured and model-elaborated process variables [5,9,21].

The three on-line self-diagnostics methods described in this paper are:

- "energy model-based diagnostics": based on the "mass–spring" localization algorithm [22];
- "distance model-based diagnostics": based on the use of a distance reference standard embedded in the system;
- "sensor physical diagnostics": based on the redundancy of Crickets' US transceivers.

The basic principle of all these methods is to define an acceptance interval. If the measurement value (*y*) is included in this interval, the acceptance test gives a positive response.

For each measurement, if all these three tests are satisfied at once, the measured result is considered reliable. Otherwise, the measurement is rejected.

After a general description of MScMS, the paper focuses on these three on-line diagnostics tools. For each method a numerical example is presented and discussed. The following aspects are analyzed in detail: theoretical description of each test, empirical definition of the test parameters and acceptance limits, trial runs and preliminary experimental results, critical aspects and possible improvements.

3. MScMS technological and operating features

MScMS prototype is made up of three main components (see Fig. 1) [6]:

- a constellation (network) of wireless devices (Crickets), opportunely arranged around the working area;
- a measuring probe, communicating via ultrasound transceivers (US) with constellation devices in order to obtain the coordinates of the touched points;
- a computing and controlling system (PC), receiving and processing data sent by the mobile probe, in order to evaluate objects geometrical features.

The measuring probe is a mobile system hosting two wireless devices, a tip to touch the surface points of the measured objects and a trigger to activate data acquisition (see Fig. 2) [6].

Given the geometrical characteristics of the mobile probe, the tip coordinates can be univocally determined by means of the spatial coordinates of the two probe Crickets [6].

Crickets are developed by Massachusetts Institute of Technology and Crossbow Technology Inc. They utilize one radiofrequency (RF) and two ultrasound (US) transceivers in order to communicate and evaluate mutual distances (see Fig. 3) [23]. Mutual distances are estimated by a technique known as TDoA (Time Difference of Arrival) [24]. The RF communication makes each Cricket rapidly know the distances among other devices. A Bluetooth transmitter connected to one of the two probe's Crickets sends this distance information to the PC, equipped with an ad hoc software to elaborate them.

The system makes it possible to calculate the position – in terms of spatial coordinates – of the object points "touched" by the probe. More precisely, when the trigger mounted on the mobile probe is pulled, current distances between the probe Crickets and the constellation ones are sent to the PC. Acquired data are utilized for the calculation of the touched point coordinates. In this way, different types of elaborations can be performed: determination of distances, geometrical tolerances, geometrical curves or object surfaces [6].

Constellation devices (Crickets) operate as reference points (beacons) for the mobile probe. Spatial location and calibration of the constellation devices are made up by a specific procedure using a "trilateration" technique [6,25,26].

To uniquely determine the relative location of a point on a 3D space, at least 4 reference points are generally needed [27–29]. In general, a trilateration problem can be formulated as follows. Given a set of *N* nodes with known coordinates (x_i, y_i, z_i, where $i = 1...N$) and a set of measured distances d_{M_i} from a generic point $P \equiv (x_P, y_P, z_P)$, the following system of non-linear equations needs to be solved to calculate the unknown coordinates (x_P, y_P, z_P) of *P* (see Fig. 4):

$$\begin{bmatrix} (x_1 - x_P)^2 + (y_1 - y_P)^2 + (z_1 - z_P)^2 \\ (x_2 - x_P)^2 + (y_2 - y_P)^2 + (z_2 - z_P)^2 \\ \vdots \\ (x_N - x_P)^2 + (y_N - y_P)^2 + (z_N - z_P)^2 \end{bmatrix} = \begin{bmatrix} d_{M_1}^2 \\ d_{M_2}^2 \\ \vdots \\ d_{M_N}^2 \end{bmatrix} \quad (1)$$

If this trilateration problem is over defined (4 or more reference points are available), it can be solved using a least-mean squares approach [30].

The position of each unknown node can be estimated by performing the iterative minimization of the following Error Function

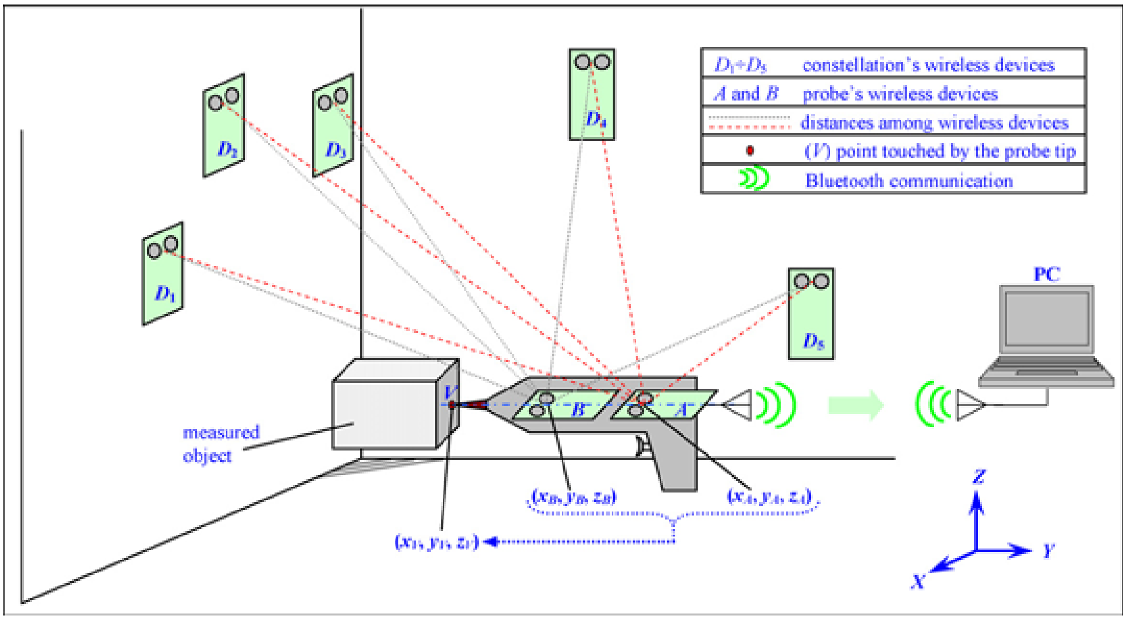

Fig. 1. MScMS working scheme.

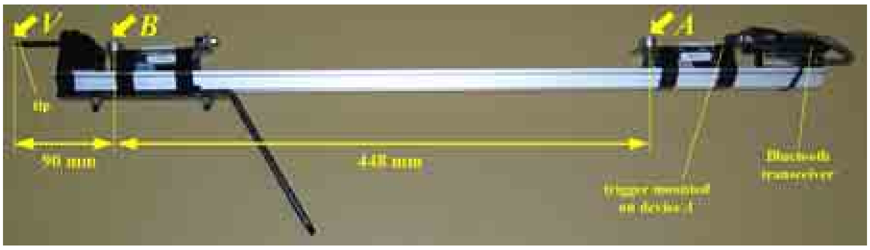

Fig. 2. Mobile probe prototype. The distance between the two probe devices is a construction parameter defined during the probe design phase.

($EF(\vec{x}_P)$) [6]:

$$EF(\vec{x}_P) \equiv \frac{\sum_{i=1}^{N}(d_{C_i} - d_{M_i})^2}{N} \quad (2)$$

being: N, the number of a priori known reference points (vectors $\vec{x}_i = (x_i, y_i, z_i)$, $i = 1\ldots N$); $\vec{x}_P = (x_P, y_P, z_P)$, the point P unknown coordinates in the localization space $\xi \subseteq \Re^3$; d_{M_i}, the measured distances between the i-th reference point and P; d_{C_i}, the Euclidean distance between the i-th reference point and P:

$$d_{C_i} = \sqrt{(x_P - x_i)^2 + (y_P - y_i)^2 + (z_P - z_i)^2} \quad (3)$$

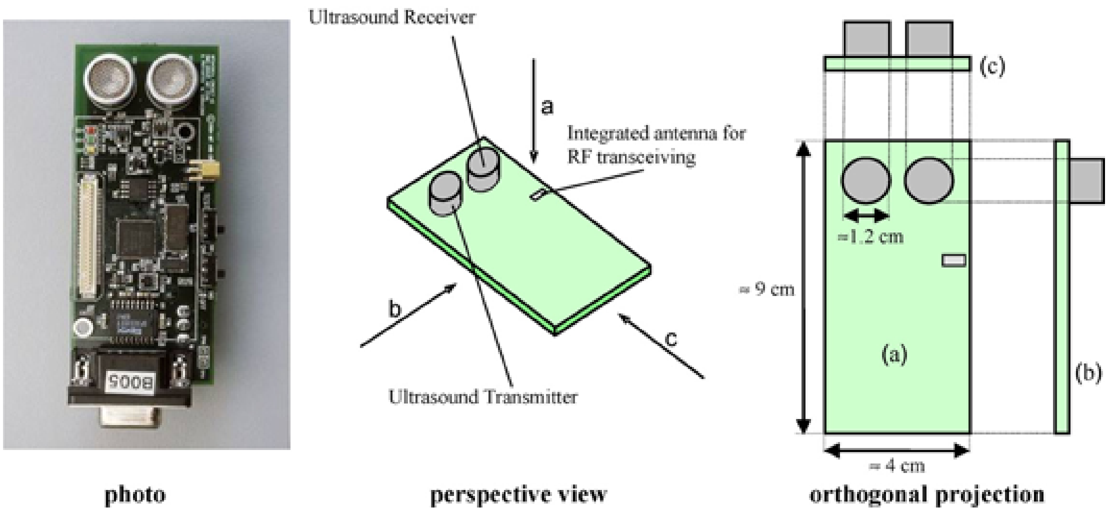

Fig. 3. Cricket structure.

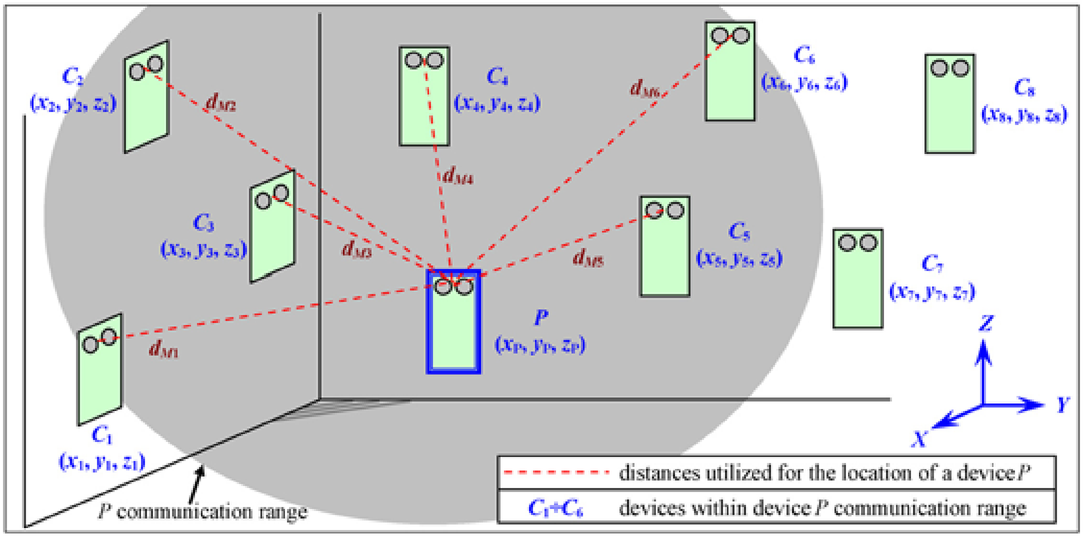

Fig. 4. Location of a generic device *P*.

The problem of finding a minimum for the function $EF(\vec{x}_P)$ can be seen as the problem of finding the point of equilibrium for a mass–spring system (lowest potential energy) [22,31].

As an example, let consider the 2D configuration described in Fig. 5. A unitary mass is associated to each network node. The node with an unknown position is connected to three reference nodes by three springs. Each of these has a rest length equal to the measured distance and a unitary force constant.

Knowing the rest lengths (d_{M_i}) and the masses positions, the system potential energy is given by

$$U(\vec{x}_P) = \sum_{i=1}^{N} \frac{1}{2}\left(\sqrt{(x_P - x_i)^2 + (y_P - y_i)^2} - d_{M_i}\right)^2 \tag{4}$$

Fig. 6(a) and (b), respectively show a 3D and 2D visualization of $EF(\vec{x}_P)$. Since $EF(\vec{x}_P) \propto U(\vec{x}_P)$, they have the same minima. As expected, the global minimum is where the node to be located actually is ($P \equiv (-10; 0)$).

4. MScMS diagnostic system

Being based upon US technology, MScMS is sensible to many influencing factors. US signals may be diffracted and reflected by obstacles interposed between two devices, external uncontrolled events can become undesirable US wave sources and even positioning algorithms can lead to non-acceptable solutions. These and other potential causes of accidental measurement errors must be taken under control to assure proper levels of accuracy.

With the aim of protecting the system, MScMS implements a series of statistical tests for on-line diagnostics. Three of them are analyzed in the following sections:

- "energy model-based diagnostics";
- "distance model-based diagnostics";
- "sensor physical diagnostics".

5. Test 1: Energy model-based diagnostics

By definition (Eq. (2)), $EF(\vec{x}_P) \geq 0$ for all $\vec{x}_P \in \xi$. In particular, $EF(\vec{x}_P) = 0$ when $d_{M_i} = d_{C_i}$, for $i = 1 \ldots N$. Because of the measuring instrument natural variability, two typical situations may occur:

- $EF(\vec{x}_P)$ is strictly positive even in the point of correct localization;
- $EF(\vec{x}_P)$ shows a global minimum in a point that is not the correct one. In other words, due to the "noise" in distance measurements, a local minimum may turn into a global minimum and vice-versa.

The energy model-based diagnostics introduces a criterion to identify all the non-acceptable minima solutions for $EF(\vec{x}_P)$, in order to prevent system fails. Such criterion enables MScMS system to distinguish between reliable and unreliable measurement.

Let consider a solution $\vec{x}_P^*$ to the problem $\min_{\vec{x}_P \in \xi} EF(\vec{x}_P)$. In general, if the problem is overdetermined (i.e., more than three distances constraints in the 3D case and more than two for the 2D case) and single measurements are affected by noise, the solution satisfying all distance constrains at the same time does not exactly fit the real node location (see Fig. 7).

In these conditions, the difference between measured and Euclidean distances are defined as residuals ($\varepsilon_i \equiv (d_{M_i} - d_{C_i})$). In general, in absence of systematic error causes, it is reasonable to hypothesize a normal distribution for the random variables ε_i, i.e.:

$$\varepsilon_i \equiv (d_{M_i} - d_{C_i}) \sim N(0, \sigma_i^2)$$

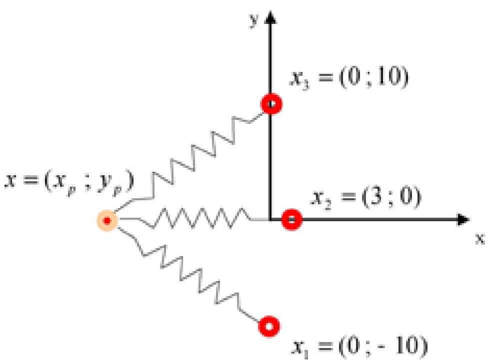

Fig. 5. An example of 2D mass–spring system. Three reference nodes ($\vec{x}_1, \vec{x}_2, \vec{x}_3$) with known position are linked by springs to the point to be localized ($\vec{x}_P$).

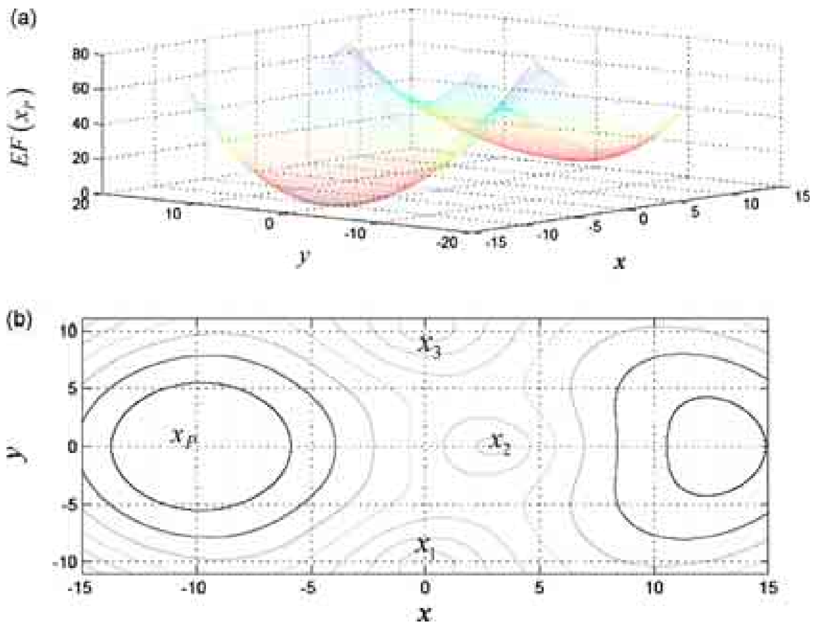

Fig. 6. (a) $EF(\vec{x}_P)$ behaviour for the mass–spring system described in Fig. 5. Finding the point of minimum means to localize the node P with unknown position. (b) Iso-energetic curves for the mass–spring system described in Fig. 5. Let notice that $\vec{x}_P$ is the global minimum point of potential energy. Maxima are in correspondence of the reference points ($\vec{x}_1, \vec{x}_2, \vec{x}_3$). Black curves refer to low energy level, grey curves refer to high energy level.

If $\sigma_i = \sigma$, $\forall i$ (this is true in absence of spatial/directional effects), Eq. (2) becomes:

$$EF(\vec{x}_P) = \sum_{i=1}^{N} \frac{(d_{M_i} - d_{C_i})^2}{N} = \sum_{i=1}^{N} \frac{\varepsilon_i^2}{N} = \frac{\sigma^2}{N} \cdot \sum_{i=1}^{N} \frac{\varepsilon_i^2}{\sigma^2} = \frac{\sigma^2}{N} \cdot \sum_{i=1}^{N} \left(\frac{\varepsilon_i}{\sigma}\right)^2 = \frac{\sigma^2}{N} \cdot \sum_{i=1}^{N} z_i^2 \qquad (5)$$

Eq. (5) can be seen as the sum of the squares of N normally distributed random variables with mean 0 and variance 1, multiplied by the constant term σ^2/N.

It must be highlighted that the sum in Eq. (5) has only $(N-1)$ independent terms. Eq. (5) causes the loss of a degree of freedom. This implies that, once $(N-1)$ terms are known, the N-th one is univocally determined.

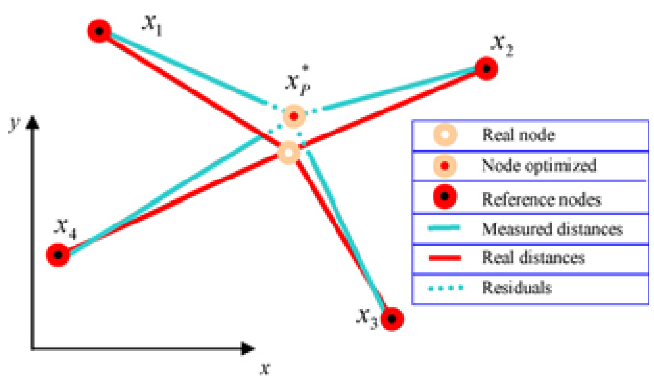

Fig. 7. An example of possible node localization. Measured distances are not equal to real distances.

Defined χ_P^2 as

$$\chi_P^2 = \sum_{i=1}^{N} \left(\frac{\varepsilon_i}{\sigma}\right)^2$$

$EF(\vec{x}_P)$ in Eq. (5) has a chi-square distribution with $N-1$ degrees of freedom:

$$EF(\vec{x}_P) = \frac{\sigma^2}{N} \cdot \chi_P^2 \qquad (6)$$

The residual standard deviation σ can be a priori estimated for the whole measuring space, for example, during the phase of installation and calibration of the system.

Every time a measurement is performed for each probe Cricket, MScMS diagnostics computes the following quantity:

$$\chi_P^{2*} = EF(\vec{x}_P^*) \frac{N}{\sigma^2} \qquad (7)$$

Assuming a risk α as a type I error, a one-sided confidence interval for variable $\chi_{\nu,\alpha}^2$ can be calculated. $\chi_{\nu,\alpha}^2$ is a chi-square distribution with $\nu = (N-1)$ degrees of freedom and a $(1-\alpha)$ confidence coefficient. The confidence interval is assumed as the acceptance interval for the reliability test of the measurement.

The test drives to the following two alternative conclusions:

- $\chi_P^{2*} \le \chi_{\nu,\alpha}^2$: the measurement is not considered unreliable, hence it is not rejected;
- $\chi_P^{2*} > \chi_{\nu,\alpha}^2$: the measurement is considered unreliable, hence it is rejected and the operator is asked to perform another one.

It is important to highlight that this test can be applied in many other different contexts in which trilateration or triangulation are utilized for coordinate measurement (3rd Tech Hi-Ball, Leica T-Probe, Metris Laser Radar and i-GPS, etc.) [32,33].

5.1. Set-up of test 1 parameters

The risk level α is established by the user depending on the required level of performance of the system. A high level of α prevents from non-acceptable solutions of the optimization problem, minimizing type II error level β.

On the other hand, a low level of α speeds up the measurement procedure, although it might drive to collect wrong data due to the high level of type II error β [34].

The residual standard deviation σ can be evaluated in two ways:

- By applying the uncertainty composition law to the coordinates calculation, starting from the measurement uncertainty of the distances between constellation beacons and probe crickets [17].
- Empirically, on the basis of experimental distance measurements. In this case, σ is estimated from a sample of residuals obtained by measuring a set of points randomly distributed in the whole working volume. This method requires the a priori knowledge of the position of the measured points. It can be easily implemented during the initial phase of setting up and calibration of the system.

In the following we focus on this second method.

Given a set of M points distributed in the measurement space $\xi \subseteq \Re^3$, randomly measured by a single Cricket (i.e., with a random sequence of measurement and a random positioning and orientation of the Cricket), for each point j a set of N_j residuals can be calculated ($j = 1\ldots M$).

It must be highlighted that the number of residuals N_j may change due to the different number of distances, detected during each measurement.

In absence of systematic error causes and time or spatial/directional effects, it is reasonable to hypothesize the same normal distribution for all the random variables ε_{ij} ($j = 1\ldots M$, $i = 1\ldots N_j$), i.e.:

$$\varepsilon_{ij} \equiv (d_{M_i} - d_{C_i})_j \sim N(0, \sigma^2)$$

The standard deviation σ may be estimated as follows:

$$\hat{\sigma} = \sqrt{\sum_{j=1}^{M}\sum_{i=1}^{N_j} \frac{(\varepsilon_{ij} - 0)^2}{\sum_{j=1}^{M} N_j}} = \sqrt{\sum_{j=1}^{M}\sum_{i=1}^{N_j} \frac{(\varepsilon_{ij})^2}{\sum_{j=1}^{M} N_j}} \tag{8}$$

The obtained value of $\hat{\sigma}$ is considered as the reference value for the test.

With this notation, Eq. (7) becomes:

$$\chi_P^{2*} = EF(\vec{x}_P^*) \cdot \frac{N}{\sigma^2} \cong EF(\vec{x}_P^*) \cdot \frac{N}{\hat{\sigma}^2} \tag{9}$$

5.2. An example of application of the energy model-based diagnostics

An empirical preliminary investigation has been carried out to verify the goodness of this approach.

Considering that ultrasound sensors are able to achieve uncertainties of about 10 mm on distance measurements (confidence coefficient $1 - \alpha = 0.95$, i.e., a covering factor $k \cong 2$) [17], for a network constituted of five reference points (constellation beacons), placed in the measurement volume as schematized in Fig. 8, $\hat{\sigma}$ has been empirically estimated as follows:

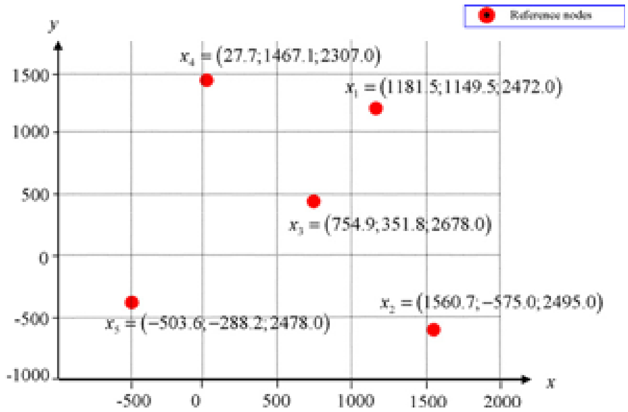

Fig. 8. Scheme of the reference node disposal (constellation beacons) in the measurement volume (point coordinates in millimetres [mm]).

- $M = 253$ points randomly distributed in the working volume have been measured by a single Cricket.
- The coordinates of each node ($\vec{x}_j$, $j = 1\ldots M$) have been evaluated using the "mass–spring" localization algorithm. A sample of 1123 residuals has been obtained.
- Normal distribution of residuals has been tested using a chi-square test [34].
- Standard deviation of residuals has been estimated by Eq. (8). The obtained result is $\hat{\sigma} = 10.0$ mm (see Table 1 for data details).

In such conditions the acceptance limit for $EF(\vec{x}_P)$, assuming a type I risk level $\alpha = 0.05$ and $\nu = (N-1) = (5-1) = 4$ degree of freedom, becomes:

$$EF(\vec{x}_P^*) \le \frac{\hat{\sigma}^2}{N} \cdot \chi^2_{\nu=4,\alpha=0.05} \Rightarrow EF(\vec{x}_P^*) \le 189\,\text{mm}^2.$$

Let now consider a typical situation that can occur using the ultrasound technology to estimate distances: US reflection. Referring to the configuration in Fig. 9, suppose that a generic point P, inside of the measurement volume (for example, $P \equiv (1067.2; -122.5; 925.8)$), has to be localized. A Cricket positioned in P is able to correctly measure distances from all the reference nodes except one of them. An obstacle (for example, the operator doing the measurement) is interposed between P and that node, preventing direct US signal propagation. At the same time, a wall placed close to the two nodes causes US signal reflection. The consequence is that the pairwise distance estimation between those two node results 100 mm larger.

Table 1
Details of data analysis for standard deviation estimation of residuals.

Sample dimension: $N_{TOT} = \sum_{j=1}^{M} N_j$	1123
Mean estimate: $\hat{\mu} = \sum_{j=1}^{M}\sum_{i=1}^{N_j} \frac{\varepsilon_{ij}}{\sum_{j=1}^{M} N_j}$	0.3 mm
Standard deviation estimate: $\hat{\sigma} = \sqrt{\sum_{j=1}^{M}\sum_{i=1}^{N_j} \frac{(\varepsilon_{ij})^2}{\sum_{j=1}^{M} N_j}}$	10.0 mm
Maximum: $\varepsilon_{MAX} = Max\{\varepsilon_{ij} \mid i = 1\ldots N_j, j = 1\ldots M\}$	42.7 mm
Minimum: $\varepsilon_{MIN} = Min\{\varepsilon_{ij} \mid i = 1\ldots N_j, j = 1\ldots M\}$	−37.1 mm

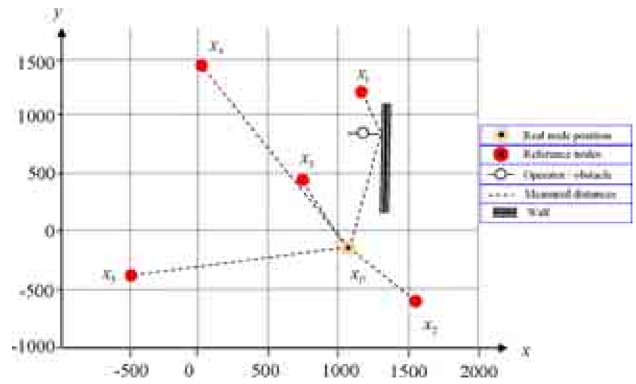

Fig. 9. Schematization of a potential misleading situation: walls and obstacles can cause wrong distances estimations (point coordinates in millimetres [mm] – see Fig. 8). In this case the measured distance between node 1 and node P results higher than the real distance.

The measured distances are:

$$d_{M_1} = 2104.8\,\text{mm}$$
$$d_{M_2} = 1713.4\,\text{mm}$$
$$d_{M_3} = 1831.4\,\text{mm}$$
$$d_{M_4} = 2355.6\,\text{mm}$$
$$d_{M_5} = 2215.2\,\text{mm}$$

In this case, the algorithm will produce the following wrong localization solution (see Fig. 10):

$$\vec{x}^*_{P'} \equiv (1022.6; -187.3; 911.8)$$

characterized by a high level of “energy”:

$$EF(\vec{x}^*_P) \cong 904\,\text{mm}^2 > 189\,\text{mm}^2$$

Owing to this result, the energy model-based diagnostics suggests rejecting the measurement.

Removing the obstacle, distance from beacon 1 becomes $d_{M_1} = 2004.8$ mm, and we obtain the correct localization solution:

$$\vec{x}^*_P \equiv (1067.2; -122.5; 925.8)$$

The new “energy” value is:

$$EF(\vec{x}^*_P) \cong 41\,\text{mm}^2 < 189\,\text{mm}^2$$

hence, $\vec{x}^*_P$ cannot be considered unreliable and the measurement is not rejected.

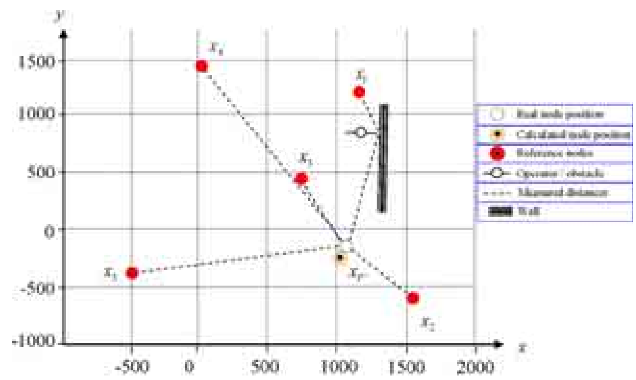

Fig. 10. Schematization of a wrong localization solution (P') due to a wrong distance estimations between node 1 and node P (point coordinates in millimetres [mm] – see Fig. 8).

6. Test 2: Distance model-based diagnostics

As described previously, the two devices (A and B) mounted on the mobile probe communicate with the constellation devices in order to estimate reciprocal distances.

The distance between the two probe devices (d_{AB}) is an a priori known design parameter (see Fig. 2). On the other hand, basing on the measured coordinates of the two devices ($\vec{x}_A$ and $\vec{x}_B$) the Euclidean distance can be easily calculated as follows:

$$\tilde{d}_{AB} = ||\vec{x}_B - \vec{x}_A|| = \sqrt{(x_A - x_B)^2 + (y_A - y_B)^2 + (z_A - z_B)^2} \tag{10}$$

Considering the following random variable (residual):

$$\varepsilon_{AB} \equiv \tilde{d}_{AB} - d_{AB} \tag{11}$$

it is reasonable to associate these residuals to a zero-mean normal distribution:

$$\varepsilon_{AB} \sim N(0, \sigma_{AB})$$

Assuming a risk α as a type I error, a further statistical test can be performed in order to evaluate measurement reliability.

Let Q_{MIN} and Q_{MAX} be the $(\alpha/2)$-quantile and $(1-(\alpha/2))$-quantile respectively of a normal distribution with mean $\mu_{AB} = 0$ and standard deviation σ_{AB}.

For a given value of α, Q_{MIN} and Q_{MAX} can be expressed as multiples of standard deviation σ_{AB}:

$$\begin{aligned} Q_{MIN} &= z_{\alpha/2} \cdot \sigma_{AB} \\ Q_{MAX} &= z_{1-(\alpha/2)} \cdot \sigma_{AB} \end{aligned} \tag{12}$$

where $z_{\alpha/2}$ and $z_{1-(\alpha/2)}$ are the values of the standard normal distribution corresponding to $\alpha/2$ and $(1-(\alpha/2))$ levels of probability respectively.

As before, standard deviation σ_{AB} can be a priori estimated, during the preliminary phase of installation and calibration of the system.

Every time a measurement is performed, MScMS diagnostics computes the following quantity:

$$\varepsilon^*_{AB} = \tilde{d}^*_{AB} - d_{AB} \tag{13}$$

The interval $[Q_{MIN}, Q_{MAX}]$ is assumed as the acceptance interval for the reliability test of the measurement.

If the calculated residual ε^*_{AB} satisfies the condition

$$Q_{MIN} \le \varepsilon^*_{AB} \le Q_{MAX} \tag{14}$$

the measurement cannot be considered unreliable, hence it is not rejected.

6.1. Set-up of test 2 parameters

As usual, the risk level α is established by the user depending on the required level of performance of the system.

Similarly to the energy model-based diagnostics, standard deviation σ_{AB} can be evaluated by applying the uncertainty composition law, or empirically, on the basis of experimental distance measurement. Here below we focus on the second method.

A set of M points randomly distributed in the measurement space $\xi \subseteq \mathfrak{R}^3$ are randomly measured. For each measurement $\varepsilon_{AB,j}$ residual is calculated (where $j = 1\ldots M$).

In the absence of systematic error causes and time or spatial/directional effects, we hypothesize the same normal distribution for all the random variables $\varepsilon_{AB,j}$, i.e.:

$$\varepsilon_{AB,j} \sim N(0, \sigma^2_{AB})$$

The standard deviation may be estimated as follows:

$$\hat{\sigma}_{AB} = \sqrt{\sum_{j=1}^{M} \frac{(\varepsilon_{AB,j} - 0)^2}{M}} = \sqrt{\sum_{j=1}^{M} \frac{(\varepsilon_{AB,j})^2}{M}} \quad (15)$$

The obtained value of $\hat{\sigma}_{AB}$ is considered as the reference value for the test.

Test limits defined in Eq. (12) become:

$$Q_{MIN} = z_{\alpha/2} \cdot \hat{\sigma}_{AB} \\ Q_{MAX} = z_{1-(\alpha/2)} \cdot \hat{\sigma}_{AB} \quad (16)$$

6.2. An example of application of the distance model-based diagnostics

Also for this approach, an empirical preliminary investigation has been carried out.

In order to estimate σ_{AB} the steps here below have been followed:

- A sample of $M = 147$ points randomly measured by the probe has been considered.
- The coordinates of each probe device have been evaluated using the "mass–spring" localization algorithm. A sample of 147 residuals has been obtained.
- Normal distribution of residuals has been tested using a chi-square test.
- Standard deviation of residuals has been estimated using Eq. (15). The obtained result is $\hat{\sigma}_{AB} = 17.3$ mm (see Table 2 for data details).

The resulting 95% confidence interval for ε_{AB} is [−34.0; 34.0] mm. A generic measurement point cannot be considered unreliable if

$$|\varepsilon^*_{AB}| \le 34.0\,\text{mm}$$

Now, let consider again the situation described Fig. 9. Suppose that Cricket A of the probe is located on point P. Due to the reflection effects, the localization algorithm produces the following incorrect coordinates of cricket A:

$$\vec{x}^*_{A'} \equiv (1022.6; -187.3; 911.8)$$

Cricket B localization is not effected by reflection error, calculated coordinates are:

$$\vec{x}^*_B \equiv (850.1; 257.9; 835.3)$$

Knowing the nominal distance $d_{AB} = 448.0$ mm (see Fig. 2), the system produces a distance residual $\varepsilon^*_{AB} = 35.5$ mm. This value is not included in the acceptance interval ([−34.0; 34.0] mm). Hence the diagnostics software of the system automatically suggests rejecting the measure.

Table 2
Details of data analysis for standard deviation estimation of residuals.

Sample dimension: $N_{TOT} = M$	147
Mean estimate: $\hat{\mu}_{AB} = \sum_{j=1}^{M} \frac{\varepsilon_{AB,j}}{M}$	−0.5 mm
Standard deviation estimate: $\hat{\sigma}_{AB} = \sqrt{\sum_{j=1}^{M} \frac{(\varepsilon_{AB,j})^2}{M}}$	17.3 mm
Maximum: $\varepsilon_{AB,MAX} = Max\{\varepsilon_j \mid j = 1 \ldots M\}$	40.7 mm
Minimum: $\varepsilon_{AB,MIN} = Min\{\varepsilon_j \mid j = 1 \ldots M\}$	−40.5 mm

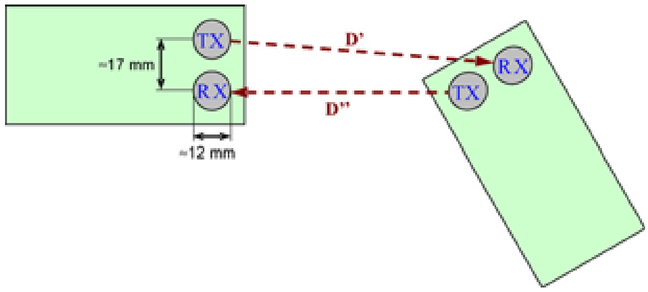

Fig. 11. Schematic representation of the difference between "received" and "transmitted" distances for two Crickets.

As above, if the obstacle is removed, the new coordinates of A become:

$$\vec{x}^*_A \equiv (1067.2; -122.5; 925.8)$$

The new residual is $\varepsilon^*_{AB} = -0.8$ mm, therefore the measurement is not rejected.

7. Test 3: Sensor physical diagnostics

Cricket devices are provided with two ultrasound sensors: a transmitter and a receiver (see Fig. 3). This allows each device to compute two different distances (d_T and d_R) related to transmitted and received US signals respectively.

Fig. 11 shows how the two measured distances can assume different values depending on the orientation of devices. Distances estimated by US signal received are used as a further redundancy.

Also in this case it is possible to study the distribution of the difference between these two measures of distance in order to establish a diagnostic criterion. The following random variable is defined (residual):

$$\varepsilon_{TR} \equiv d_T - d_R \quad (17)$$

As a first approximation:

$$\varepsilon_{TR} \sim N(0, \sigma_{TR})$$

Assuming a risk α as a type I error, a statistical test can be performed in order to evaluate measurement reliability.

Acceptance interval limits are defined in the same way as for the distance model-based diagnostics:

$$Q_{MIN} = z_{\alpha/2} \cdot \sigma_{TR} \\ Q_{MAX} = z_{1-(\alpha/2)} \cdot \sigma_{TR} \quad (18)$$

Since MScMS requires the simultaneous localization of devices A and B (see Fig. 2), at least eight distances are evaluated at the same time. We remind that four distances are necessary to locate a point in a 3D space. If the calculated residual for each measured distance lies in the confidence interval then the measurement cannot be considered unreliable and it is not rejected, otherwise the system asks to reject the measurement. The following condition must be verified:

$$Q_{MIN} \le \varepsilon^*_{TR,i} \le Q_{MAX}, \forall i \in \{1 \ldots N\} \quad (19)$$

where N is the number of constellation beacons communicating with a given probe device (residuals) defined every time a measurement is performed.

7.1. Set-up of test 3 parameters

As usual, the risk level α is established by the user depending on the required level of performance of the system.

Similarly to the two diagnostics models described in the previous sections, standard deviation σ_{TR} can be evaluated by applying the uncertainty composition law, or empirically, on the basis of experimental distance measurement.

Considering the second method, a set of M points randomly distributed in the measurement space $\xi \subseteq \Re^3$ are randomly measured. For each measurement $\varepsilon_{TR,ji}$ is calculated (where $i = 1 \ldots N_j$ and $j = 1 \ldots M$). The number of residuals N_j may change due to the different number of distances, detected during each measurement.

Hypothesizing a normal distribution for all the random variables $\varepsilon_{TR,ji}$, i.e.:

$$\varepsilon_{TR,ji} \sim N(0, \sigma_{TR}^2)$$

The standard deviation may be estimated as follows:

$$\hat{\sigma}_{TR} = \sqrt{\sum_{i=1}^{N}\sum_{j=1}^{M} \frac{(\varepsilon_{TR,ji} - 0)^2}{\sum_{j=1}^{M} N_j}} = \sqrt{\sum_{i=1}^{N}\sum_{j=1}^{M} \frac{(\varepsilon_{TR,ji})^2}{\sum_{j=1}^{M} N_j}} \quad (20)$$

The obtained value of $\hat{\sigma}_{TR}$ is considered as the reference value for the test.

Test limits defined in Eq. (18) become:

$$\begin{aligned} Q_{MIN} &= z_{\alpha/2} \cdot \hat{\sigma}_{TR} \\ Q_{MAX} &= z_{1-(\alpha/2)} \cdot \hat{\sigma}_{TR} \end{aligned} \quad (21)$$

7.2. An example of application of the distance model-based diagnostics

Also for this kind of diagnostics an application example is reported.

In order to estimate σ_{TR} the steps here below have been followed:

- A sample of $M = 30$ points randomly measured by the probe has been considered.
- The coordinates of each probe device have been evaluated using the "mass–spring" localization algorithm. A sample of 254 residuals has been obtained.
- Normal distribution of residuals has been tested using a chi-square test.
- Standard deviation of residuals has been estimated using Eq. (20). The obtained result is $\hat{\sigma}_{AB} = 12.9$ mm (see Table 3 for data details).

The resulting 95% confidence interval for ε_{TR} is [−25.3; 25.3] mm. Therefore a generic point measurement cannot be considered unreliable if

$$\left|\varepsilon^*_{TR,i}\right| \leq 25.3\,\text{mm} \quad \forall i \in \{1 \ldots N\}$$

where $\varepsilon^*_{TR,i}$ is the calculated value of residual during a specific measurement.

Table 3
Details of data analysis for standard deviation estimation of residuals.

Sample dimension: $N_{TOT} = \sum_{j=1}^{M} N_j$	254
Mean estimate: $\hat{\mu}_{TR} = \sum_{i=1}^{N}\sum_{j=1}^{M} \frac{\varepsilon_{TR,ji}}{\sum_{j=1}^{M} N_j}$	0.6 mm
Standard deviation estimate: $\hat{\sigma}_{TR} = \sqrt{\sum_{i=1}^{N}\sum_{j=1}^{M} \frac{(\varepsilon_{TR,ji})^2}{\sum_{j=1}^{M} N_j}}$	12.9 mm
Maximum: $\varepsilon_{TR,MAX} = Max\{\varepsilon_{TR,ji} \mid i = 1 \ldots N_j, j = 1 \ldots M\}$	32.3 mm
Minimum: $\varepsilon_{TR,MIN} = Min\left\{\varepsilon_{TR,ji} \mid i = 1 \ldots N_j,\ j = 1 \ldots M\right\}$	−27.3 mm

Consider the situation described in Fig. 9, where the Cricket A of the probe is located on point P.

The measured distances in reception are:

$$\begin{aligned} d_{R_1} &= 2104.8\,\text{mm} \\ d_{R_2} &= 1713.4\,\text{mm} \\ d_{R_3} &= 1831.4\,\text{mm} \\ d_{R_4} &= 2355.6\,\text{mm} \\ d_{R_5} &= 2215.2\,\text{mm} \end{aligned}$$

The measured distances in transmission are:

$$\begin{aligned} d_{T_1} &= 2136.2\,\text{mm} \\ d_{T_2} &= 1695.5\,\text{mm} \\ d_{T_3} &= 1818.7\,\text{mm} \\ d_{T_4} &= 2357.7\,\text{mm} \\ d_{T_5} &= 2221.9\,\text{mm} \end{aligned}$$

Due to the reflection effect we observe a significant difference between the two distances measured from beacon 1. We obtain the following residual values:

$$\begin{aligned} \varepsilon^*_{TR,1} &= 31.4\,\text{mm} \\ \varepsilon^*_{TR,2} &= -17.9\,\text{mm} \\ \varepsilon^*_{TR,3} &= -12.7\,\text{mm} \\ \varepsilon^*_{TR,4} &= 2.1\,\text{mm} \\ \varepsilon^*_{TR,5} &= 6.7\,\text{mm} \end{aligned}$$

Since residual 1 value is not included in the acceptance interval ([−25.3; 25.3] mm), the diagnostics test suggests rejecting the measurement.

8. Conclusion

MScMS is an innovative wireless measuring system complementary to CMMs. A prototype of this system has been developed at the industrial metrology and quality engineering laboratory of DISPEA – Politecnico di Torino. It is portable, not too much expensive, and suitable for large-scale metrology (uneasy on conventional CMMs).

Some innovative aspects of the system concern its on-line diagnostics tools. When dealing with measurement systems, the importance of a good diagnostics of produced measures is crucial for applications in which errors can lead to serious consequences.

The diagnostics tools described in this paper, all based on the concept of "reliability of a measurement", enable MScMS user to reject measurements which do not satisfy a series of statistical acceptance tests with a given confidence coefficient.

For each measurement, if all these tests are satisfied at once, the measured result is considered acceptable. Otherwise, the measurement is rejected.

After rejection, the operator is asked to redo the measurement, changing the orientation/positioning of the probe or, if it is necessary, beacons arrangement in the system network.

In same cases, the system might force to repeat a measurement too many times, causing an excessive extension of the measurement duration. This problem can be overcome by changing the configuration of the constellation.

Future work, as well as improving the power of the existing tools, will be aimed to enrich MScMS control system by implementing additional tools able to steer the operator during measurement. For example, suggesting the position of the probe in the measuring volume, or proposing possible extensions of the network of beacons, or automatically filtering and/or correcting corrupted measurements.

References

[1] Bosch JA. Coordinate measuring machines and systems. Marcel Dekker Inc.; 1995. ISBN 0-8247-9581-4.

[2] Cauchick-Miguel P, King T, Davis J. CMM verification: a survey. Measurement 1996;17(1):1–16.
[3] Hansen HN, De Chiffre L. An industrial comparison of coordinate measuring machines in Scandinavia with focus on uncertainty statements. Precision Engineering 1999;23(3):185–95.
[4] Franceschini F, Galetto M, Maisano. Management by measurement. Designing key indicators and performance measurement systems. Berlin: Springer-Verlag; 2007. ISBN: 978-3-540-73211-2.
[5] Franceschini F, Galetto M. A taxonomy of model-based redundancy methods for CMM on-line performance verification. International Journal of Technology Management 2007;37(1-2):104–24. Special Issue: Innovation behind quality: the innovation challenge for Quality methods and tools.
[6] Franceschini F, Galetto M, Maisano D, Mastrogiacomo L. Mobile Spatial coordinate Measuring System (MScMS) – introduction to the system. International Journal of Production Research, forthcoming.
[7] ISO 10360-2. Geometrical Product Specifications (GPS) – acceptance and reverification tests for coordinate measuring machines (CMM). Part 2: CMMs used for measuring size. Geneva, Switzerland: International Organization for Standardization; 2001.
[8] Hofmann-Wellenhof B, Lichtenegger H, Collins J. GPS. Theory and practice. Wien, Austria: Springer; 2001.
[9] Gertler JJ. Fault detection and diagnosis in engineering system. New York: Marcel Dekker; 1998.
[10] ISO/TS 15530-4. Geometrical Product Specifications (GPS) – coordinate measuring machines (CMM): technique for determining the uncertainty of measurement. Part 4: evaluating task-specific measurement uncertainty using simulation. Geneva, Switzerland: International Organization for Standardization; 2008.
[11] ISO/TS 15530-3. Geometrical Product Specifications (GPS) – coordinate measuring machines (CMM): technique for determining the uncertainty of measurement. Part 3: use of calibrated workpieces or standards. Geneva, Switzerland: International Organization for Standardization; 2004.
[12] Phillips SD, Sawyer D, Borchardt B, Ward D, Beutel DE. A novel artifact for testing large coordinate measuring machines. Precision Engineering 2001;25(1):29–34.
[13] Savio E, Hansen HN, De Chiffre L. Approaches to the calibration of freeform artefacts on coordinate measuring machines. In: Annals of CIRP 51/1. 2002. p. 433–6.
[14] Piratelli-Filho A, Di Giacomo B. CMM uncertainty analysis with factorial design. Precision Engineering 2003;27(3):283–8.
[15] Feng CXJ, Saal AL, Salsbury JG, Ness AR, Lin GCS. Design and analysis of experiments in CMM measurement uncertainty study. Precision Engineering 2007;31(2):94–101.
[16] VIM. International vocabulary of basic and general terms in metrology. Geneva, Switzerland: International Organization for Standardization; 2004.
[17] GUM. Guide to the expression of uncertainty in measurement. Geneva, Switzerland: International Organization for Standardization; 2004.
[18] Clarke DW. Sensor, actuator, and loop validation. Ieee Control Systems Magazine 1995;15:39–45.
[19] Henry MP, Clarke DW. The self-validating sensor: rationale, definitions and examples. Control Engineering Practice 1992;1:585–610.
[20] Isermann R. Process fault detection based on modeling and estimation methods - A survey. Automatica 1984;20:387–404.
[21] Reznik LK, Solopchenko GN. Use of a-priori information on functional relations between measured quantities for improving accuracy of measurement. Measurement 1985;3(3):98–106.
[22] Franceschini F, Galetto M, Maisano D, Mastrogiacomo L. A review of localization algorithms for distributed wireless sensor networks in manufacturing. International Journal of Computer Integrated Manufacturing, forthcoming.
[23] MIT Computer Science and Artificial Intelligence Lab (2004) Cricket v2 User Manual. http://cricket.csail.mit.edu/v2man.html.
[24] Gustafsson F, Gunnarsson F. Positioning using time difference of arrival measurements. In: Proceedings of the IEEE international conference on acoustics, speech, and signal processing (ICASSP 2003), vol. 6. 2003. p. 553–6.
[25] Lee MC, Ferreira PM. Auto-triangulation and auto-trilateration. Part 1. Fundamentals. Precision Engineering 2002;26(3):237–49.
[26] Lee MC, Ferreira PM. Auto-triangulation and auto-trilateration—part 2: three-dimensional experimental verification. Precision Engineering 2002; 26(3):250–62.
[27] Chen M, Cheng F, Gudavalli R. Precision and accuracy in an indoor localization system. In: Technical Report CS294-1/2. Berkeley, USA: University of California; 2003.
[28] Sandwith S, Predmore R. Real-time 5-micron uncertainty with laser tracking interferometer systems using weighted trilateration. In: Proceedings of 2001 Boeing large scale metrology seminar. 2001.
[29] Akcan H, Kriakov V, Brönnimann H, Delis A. GPSFree node localization in mobile wireless sensor networks. In: Proceedings of MobiDE'06. 2006.
[30] Savvides A, Han C, Strivastava MB. Dynamic fine-grained localization in ad hoc networks of sensors. In: Proceedings of ACM/IEEE 7th annual international conference on mobile computing and networking (MobiCom'01). 2001. p. 166–79.
[31] Moore D, Leonard J, Rus D, Teller SS. Robust distributed network localization with noisy range measurements. In: Proceedings of SenSys 2004. 2004. p. 50–61.
[32] Welch G, Bishop G, Vicci L, Brumback S, Keller K. High-performance wide-area optical tracking the hiball tracking system. In Presence: Teleoperators And Virtual Environments 2001;10(1):1–21.
[33] Rooks B. A vision of the future at TEAM. Sensor Review 2004;24(2):137–43.
[34] Montgomery DC. Introduction to statistical process control. New York: J. Wiley; 2005.